Entropic Effects and Slow Kinetics Revealed in Titrations of D_2O-H_2O Solutions with Different D/H Ratios

Yael Katsir,[†,‡] Yoash Shapira,*[,‡] Yitzhak Mastai,[†] Rumiana Dimova,[§] and Eshel Ben-Jacob*[,‡]

Chemistry Department, Bar-Ilan University, Ramat-Gan 52900, Israel, School of Physics and Astronomy, Tel-Aviv University, Tel-Aviv 69978, Israel, and Department of Theory and Bio-Systems, Max Plank Institute of Colloids and Interfaces, Science Park Golm 14424, Germany

Received: October 8, 2009; Revised Manuscript Received: March 22, 2010

There is much renewed interest in the arrangement and kinetic of hydrogen bonds in water and heavy water. D_2O forms a higher average number of hydrogen bonds per molecule (10% more) compared to the case for H_2O, which cause a larger entropic cost for solvating molecules in D_2O. Here we used isothermal titration calorimetry (ITC) to investigate the enthalpy of titration of D_2O-H_2O solutions with different D/H isotope ratios. We found significant enthalpy deviations (exothermic contributions) relative to the computed enthalpy for the limit of ideal mixing both for dilution titration and for concentration titration (injection of solutions with lower D/H ratios into solutions with higher ratios and vice versa). We propose that the observed exothermic deviations might be connected to entropic effects associated with differences in the H and D arrangements that depend on the D/H ratio of the solutions. This ratio varies during the titration processes, leading to the entropy production beyond that of ideal mixing. We also used the ITC in the nonstirring mode to measure the titration kinetics and found long relaxation times of up to tens of minutes for the concentration titrations (but not for the dilution titrations). These observations are consistent with slow propagation of the reaction $H_2O + D_2O \leftrightarrow 2HDO$ that involves hopping of deuterium and rearrangements of the H and D bonding.

Introduction

Water, the most complex and challenging natural substance, exhibits different behavior from that of other liquids with similar chemical bondings.[1–6] Much experimental and theoretical effort has been devoted over the years to characterize and study water anomalies. More recently, several mechanisms related to chains and networks of hydrogen bonds,[7,8] low and high density water,[9,10] and the role of ortho- and para- water have been proposed[11–13] as possible mechanisms to explain water anomalies. Yet there is no agreed upon mechanisms and the origin of water anomalies is still a mystery posing one of the most fundamental open questions in physics and chemistry.[14,15]

The studies presented here are motivated by the anomalous differences between ordinary H_2O water and the D_2O heavy water in terms of the material properties, transport coefficients, and kinetic processes.[16] The measured differences significantly exceed those expected on the basis of the mass (atomic weight) difference between the two isotopes (the atomic weight of deuterium is $M_D = 2.014$ g/mol, and of hydrogen is $M_H = 1.008$ g/mol). In particular, the current research has been geared toward macroscopic thermodynamic investigation of effects associated with the changes in the arrangements of the hydrogen bonds in H_2O-D_2O solutions as a function of the D/H ratio.

Previous studies investigated the effect of the lower volume packing density of D_2O compared to that in H_2O on the physicochemical properties of nonpolar and polar solutes in H_2O-D_2O solutions.[17,18] The results were related to the higher average number of hydrogen bonds per molecule (10% more) in D_2O compared to the number of bonds in H_2O. It was proposed that the excess bonds generate entropic effects reflected in a larger entropic cost[19] for solvating molecules in D_2O and bond rearrangements in H_2O-D_2O solutions in comparison to those in pure water.[20–27]

It is reasonable to expect that the excess bond number and bond rearrangements (if existing) should also be reflected in the enthalpy of mixing of H_2O-D_2O solutions with different D/H ratios. To be more specific, H_2O-D_2O solutions are composed of three components, H_2O, D_2O, and HDO. For a solution with a given D/H ratio, the molar ratio between these three constituents is governed by the reaction constant of the endothermic reaction: $H_2O + D_2O \leftrightarrow 2HDO$. Therefore, the heat production during the titration of H_2O-D_2O solutions with different D/H ratios, ΔQ_{Reac}, includes two contributions: (1) the reaction enthalpy contribution ΔH_R and (2) the entropy contribution ΔS_{Order}, associated with the changes in the bulk entropy of H_2O-D_2O solutions with different D/H ratios.

The heat production during titration, ΔQ_{Reac} is proportional to the change in the number of moles of HDO molecules during the mixing, Δn_{HD}, multiplied by the molar enthalpy of the reaction ΔH_R. In previous studies[28] using heat flux calorimetry, the endothermic enthalpy of the reaction ΔH_R, was computed to be equal to 15.5 cal/mol of HDO formation and was found to be temperature independent in the range 298−373 K. It is important to emphasize that the enthalpy of the reaction was computed from the measured heat of mixing assuming ideal mixing (mixing of ideal solutions). In other words, entropy contributions to the heat production during the titration, are associated with deviations from ideal mixing.

Hence, ΔS_{Order} is associated with entropy changes that deviate from those that correspond to the case of ideal mixing. Such changes are likely to be associated with differences of the bulk entropy between H_2O-D_2O solutions with different D/H ratios.

* To whom correspondence should be addressed. Tel: +97236407845. Fax: +97236425787. E-mail: Y.S., yoashs@zahav.net.il; E.B.-J., eshelbj@gmail.com.
† Bar-Ilan University.
‡ Tel-Aviv University.
§ Max Plank Institute of Colloids and Interfaces.

10.1021/jp909657m
Published on Web 04/09/2010

Such bulk entropy differences are presumably related to the differences in hydrogen bond arrangements according to the D/H ratios.

Since the current studies were aimed at investigating the entropic effects of D_2O-H_2O solutions, the focus was on accurate measurements of the entropy contribution ΔS_{Order}, or in other words, on the deviations from the limit of ideal mixing. To achieve the required level of accuracy, we investigated the enthalpies of mixing of the D_2O-H_2O solutions with different D/H ratios using isothermal titration calorimetry. Currently, ITC is the most sensitive method for measuring the total heat changes during mixing/reaction processes.[29–36] We performed detailed studies of both concentration and dilution titrations (titration of solutions with low D/H ratio by solutions with higher D/H ratio and vice versa) for a wide rage of solutions with different D/H ratios.

For both cases we found similar significant deviations from the limit of ideal mixing. In particular, the total measured heat of the reaction was lower than the value computed for the limit of ideal mixing. Since, as we mentioned before, the reaction is endothermic, the results indicate exothermic entropy contribution that might reflect entropic effects associated with changes in the number and arrangements of hydrogen bonds in D_2O-H_2O solutions with different D/H ratios.

In conventional protocols, also followed in our measurements of the heat of mixing, the titration process in the ITC is performed while stirring the bulk solution in the apparatus cell (that is of about 1 mL volume) to guarantee good mixing. Yet, it is also possible to use the ITC in a nonstirring mode. This mode, which is less frequently used, can yield information about the reaction kinetics, provided the kinetics is sufficiently slow. More specifically, the reaction kinetics depends on the reaction rate or the reaction propagation in the case of diffusion-limited reaction, i.e., when the diffusion rates are slower than the reaction rates.

Thus, to extract information about the reaction kinetics, we also performed ITC measurements in the nonstirring mode. These measurements were performed to substantiate the assumption that titration D_2O-H_2O solutions with different D/H ratios involves rearrangements of hydrogen bonds and to extract estimates about the typical kinetic times. We found very long kinetic times (up to tens of minutes) for concentration titrations which require diffusion of the deuterium ions and rearrangements of the hydrogen bonds in the apparatus cell. The control experiments (to test the reliability of the nonstirring mode) with dilution titrations, which require rearrangements only in the small volume of the injected aliquots, yielded fast times as expected and the same enthalpies as measured in the case of the stirring mode.

Materials and Methods

Preparation of the D_2O-H_2O Solutions. Double distilled reverse osmosis (RO) water (H_2O) with maximum conductivity of 0.05 μS/cm was mixed with purified deuterium oxide (D_2O) from Sigma-Aldrich with 99.9% purity to prepare fresh solutions for each set of experiments. The solutions were characterized by a D/H molar fraction taking into account the differences between the molar density of D_2O (0.05515 mol/mL) and H_2O (0.05535 mol/mL) at 298 K. At this temperature, the weight and molar masses of the components are 1.1044 g/mL and 20.027 g/mol for D_2O and 0.9970 g/mL and 18.015 g/mol for H_2O. We note that the exposure to air during ITC measurements and hence D−H conversion with water vapors is limited due to the apparatus design.

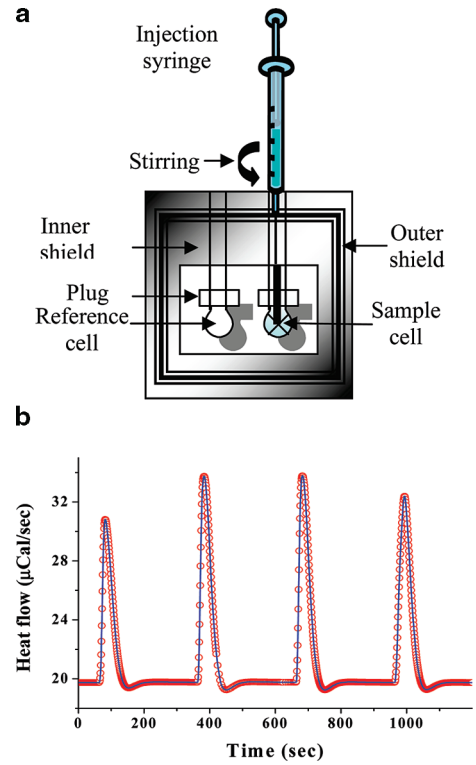

Figure 1. (a) ITC cells and syringe. (b) Reproducibility of the ITC signal demonstrated by two measurements where 20% D_2O is injected into H_2O. The two measurements (solid curve and open circles) were performed on different days. The titrations were of 5 μL aliquots at 303 K, while using high feedback and the nonstirring mode.

Isothermal Titration Calorimetry. The titration measurements were performed using the VP-ITC calorimeter of MicroCal Inc. The apparatus design, shown in Figure 1a, allows performing direct and accurate measurements of both exothermic and endothermic heat production.[29–36]

The working volume of an ITC cell, described in Figure 1, is 1.4201 mL. The volumes injected by the ITC syringe can be adjusted typically between 3 and 100 μL. The total syringe volume is about 300 μL and with a range of injection rates. Usually, the titrations are performed using the stirring mode. To assess the reaction kinetics, it is possible to perform the titrations using nonstirring mode. There is a tunable power feedback to obtain optimal sensitivity according to the measured reaction. The temperature can be selected (and then fixed) from a wide range between 278 and 356 K. During the measurements, one of the two cells, the sample and the reference cells, can be heated by thermo-power elements to maintain equal temperature between them. For an exothermic reaction (increase in the temperature of the sample cell), the reference cell is heated. Hence, in this case the sample cell is kept isolated and the relevant thermodynamic potential that describes the process is the enthalpy H. In contrast, for endothermic reaction the sample cell is heated to maintain constant temperature and hence the relevant thermodynamic potential that describes the process is the Gibbs free energy. To demonstrate the high reproducibility of the heat flow signal for endothermic processes, we show in Figure 1b two separate measurements with identical settings.

We note that the first injection is ignored as it is subject to artifacts related to the possible dilution of the solution in the syringe during the equilibration period. To extract the heat produced or absorbed during the injections, a baseline is subtracted and the peak areas are integrated over time. These analyses were performed using OriginLab built-in macros. The

experimental error is of the order of 2% and depends on the specific reaction. The precision for the measured heat for H_2O/D_2O mixing has been found to be also of the same order, as shown in the results section.

Characterization of the Solutions. The H_2O-D_2O solutions can be characterized by the deuterium mole fraction $A = n_D/(n_D + n_H)$, where n_D and n_H are the number of moles of deuterium and hydrogen atoms, respectively. As mentioned in the Introduction, the solutions are composed of three constituents: D_2O, H_2O and HDO. The mole numbers of these constituents, n_{D_2O}, n_{H_2O}, and n_{HDO}, satisfy the relations for mass conservation $n_D = 2n_{D_2O} + n_{HDO}$ and $n_H = 2n_{H_2O} + n_{HDO}$. The corresponding mole fractions of D_2O, H_2O, and HDO

$$X_D = \frac{n_{D_2O}}{n_{D_2O} + n_{HDO} + n_{H_2O}}$$

$$X_H = \frac{n_{H_2O}}{n_{D_2O} + n_{HDO} + n_{H_2O}}$$

$$X_{HD} = \frac{n_{HDO}}{n_{D_2O} + n_{HDO} + n_{H_2O}}$$

can be expressed as a function of A and the equilibrium constant, $K = 3.82$ (at 298−373 K) as determined from flow calorimetry measurements[28] of the reaction

$$H_2O + D_2O \leftrightarrow 2HDO \quad (1)$$

According to the balance relations

$$KX_DX_H = X_{HD}^2 \quad (2)$$

$$X_D + \frac{X_{HD}}{2} = A \quad (3)$$

$$X_H + \frac{X_{HD}}{2} = 1 - A \quad (4)$$

The calculated values of X_D, X_H, and X_{HD} as a function of A are shown in Figure 2a.

Reaction Heat Production. As mentioned in the Introduction, the heat production during the titration ΔQ_{Reac} includes two contributions, the reaction enthalpy ΔH_R, and the entropy contribution of deviations from ideal mixing ΔS_{Order}. Here we calculate heat production, which is proportional to Δn_{HD}, the change in the number of moles of HDO molecules during the mixing, multiplied by the enthalpy of the reaction per mole HDO, ΔH_R.

The change in the number of HDO molecules corresponds to the change in X_{HD} during a titration, which amounts to solving the quadratic equation:

$$\left(\frac{4}{K} - 1\right)X_{HD}^2 + 2X_{HD} - 4A(1 - A) = 0 \quad (5)$$

An approximated solution of this equation is presented in the Appendix.

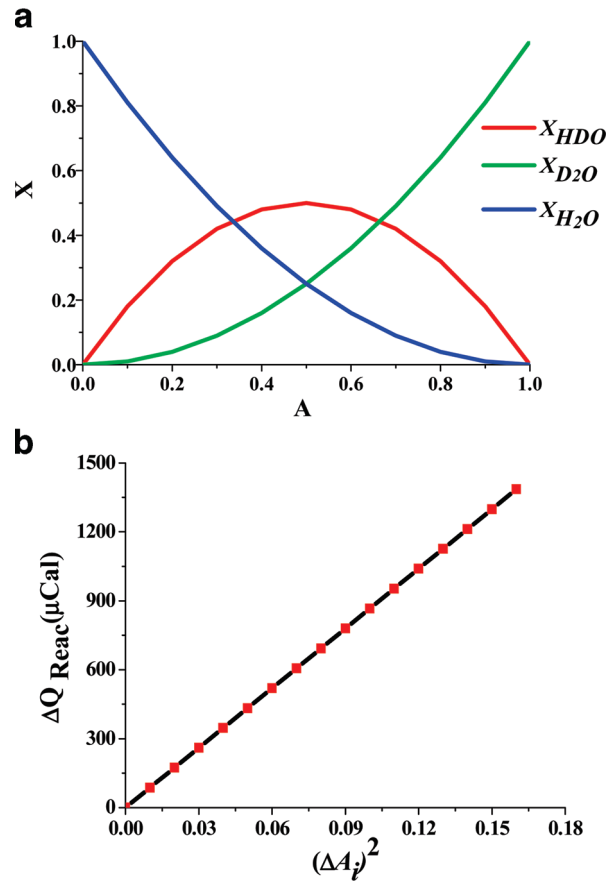

Figure 2. (a) Calculated molar fractions of D_2O (green), H_2O (blue), and HDO (red) as a function of A. (b) Calculated functional dependence of $\Delta Q_{Reac,i}$ on $(\Delta A_i)^2$. For the dilution titration ($A_{i-1} > A_{Inj}$), $\Delta Q_{Reac,i}$ are shown by red squares and for concentration titration ($A_{i-1} < A_{Inj}$) by the black line. Note that the calculated results for the two types of titrations are equal.

Since we perform several injections and following each injection the mole fractions of the three constituents change, the calculations have to be done with care. With $\Delta n_{HD,i}$ we denote the number of moles HDO produced in the measuring cell after the ith injection:

$$\Delta n_{HD,i} = X_{HD,i}n_i - X_{HD,i-1}n_{i-1} - X_{HD,Inj}n_{Inj} \quad (6)$$

Here we denote the molar fractions of HDO after the injection by $X_{HD,i}$, before the injection by $X_{HD,i-1}$, and in the injection syringe by $X_{HD,Inj}$. These molar fractions are calculated from the solution of eq 5 when we substitute for A the respective fractions A_i, A_{i-1}, and A_{Inj}. To simplify the proceeding presentation, we define

$$\Delta A_i \equiv A_{i-1} - A_{Inj} \quad (7)$$

We also note that in the dilution titrations A decreases ($A_i < A_{i-1}$), while in the concentration titrations the mole fraction A increases ($A_i > A_{i-1}$).

To calculate n_i, n_{i-1}, and n_{Inj}, we note that the total of n_{Inj} moles of H_2O, HDO, and D_2O is conserved, hence

$$n_{Inj} = V_{Inj}[\upsilon_{D_2O}\mu_{D_2O,Inj} + \upsilon_{H_2O}(1 - \mu_{D_2O,Inj})] \quad (8)$$

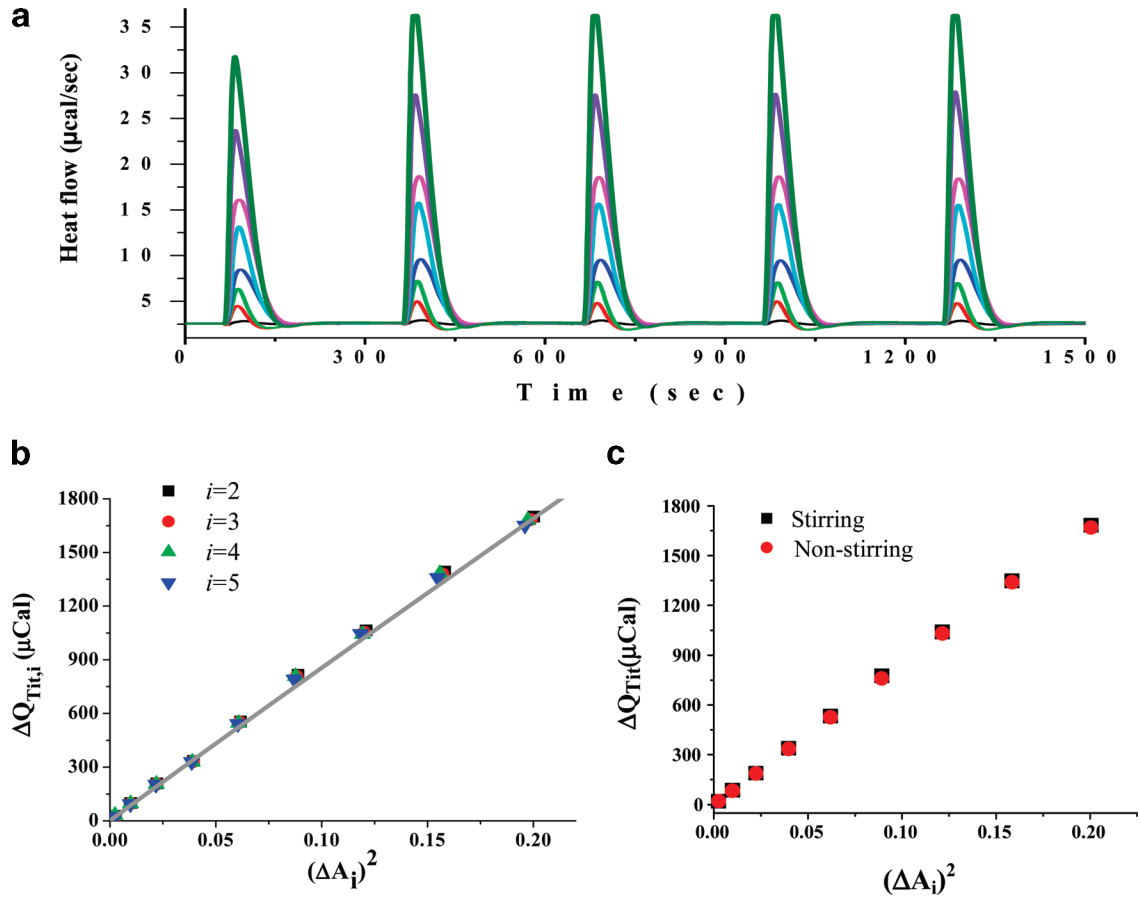

Figure 3. Experimental verification of the calculated functional dependence $\Delta Q_{\mathrm{Reac},i}$ on the mole fraction A. In (a) we show the measured heat flow during injection titrations, by 5 μL H_2O aliquots, of 8 H_2O-D_2O solutions with different D/H ratios (or different percentages of D_2O) kept in the 1.4201 mL ITC cell. The corresponding $|\Delta A_i|$ are 0.025 (black), 0.050 (red), 0.10 (green), 0.20 (blue), 0.25 (azure), 0.30 (pink), 0.35 (purple), and 0.40 (olive). The settings are 303 K, no stirring, and high feedback. (b) Total measured heat $\Delta Q_{\mathrm{Tit},i}$ of each injection (i) versus $(\Delta A_i)^2$. The gray line shows the computed heat $\Delta Q_{\mathrm{Reac},i}$. (c) Comparison between the nonstirring mode (red) and the stirring mode (black) for the 5 μL aliquots (averaged values over the injections $i = 2-5$).

where υ_{D_2O} and υ_{H_2O} are the molar densities of D_2O and H_2O, respectively ($\upsilon_{D_2O} = 0.05515$ mol/mL and $\upsilon_{H_2O} = 0.05535$ mol/mL at 298 K) and V_{Inj} is the volume of injected titrating solution. We note by $\mu_{D_2O,\mathrm{Inj}}$ the volume fraction of D_2O needed to prepare the injected solution and $1 - \mu_{D_2O,\mathrm{Inj}}$ is the volume fraction of H_2O. The total number of moles in the measuring cell before the ith injection is

$$n_{i-1} = V_0[\upsilon_{D_2O}\mu_{D_2O,0} + \upsilon_{H_2O}(1 - \mu_{D_2O,0})] + (i - 1)n_{\mathrm{Inj}} \quad (9)$$

Here V_0 is the initial volume of the solution in the measuring cell before any injection ($V_0 = 1.4201$ mL), and $\mu_{D_2O,0}$ is the volume fraction of D_2O needed to prepare the starting solution in the measurement cell. Note that in eq 9, the last term takes into account the contribution of previous injections. After the ith injection, one has in total n_i moles in the measuring cell:

$$n_i = n_{i-1} + n_{\mathrm{Inj}} \quad (10)$$

Finally, using the computed values of n_i, n_{i-1}, and n_{Inj} to calculate $\Delta n_{\mathrm{HD},i}$ in eq 5, the heat produced in the ith injection is given by

$$\Delta Q_{\mathrm{Reac},i} = \Delta n_{\mathrm{HD},i}\Delta H_R \quad (11)$$

where $\Delta H_R = 15.5$ cal/mol (at 298−373 K)[28] is the enthalpy gain for the formation of one mole of HDO.

The solution of eq 11 reveals that $\Delta Q_{\mathrm{Reac,i}}$ is linearly proportional to $(\Delta A_i)^2$, as shown in Figure 2b for both dilution and concentration case. In the Appendix we also show that

$$\Delta n_{\mathrm{HD},i} \approx [2n_{i-1}n_{\mathrm{Inj}}/(n_{i-1} + n_{\mathrm{Inj}})](\Delta A_i)^2 \quad (12)$$

For this reason we plotted the experimentally measured heat per injection, as a function of $(\Delta A_i)^2$. In this way, the deviations from the limit of ideal mixing ($\Delta Q_{\mathrm{Mix}} = \Delta Q_{\mathrm{Reac}}$) become more transparent.

Results and Discussion

Experimental Verification of ΔQ_{Reac} and ΔH_R. The expected entropy contribution $\Delta S_{\mathrm{Order}}$ which is associated with the entropic effects that deviate from ideal mixing, is expected to be significantly smaller than the released heat ΔQ_{Reac} and hence to be neglected for titrations with very low volume droplets. Therefore, to verify the calculated functional dependence ΔQ_{Reac} on the mole fraction A (eq 11) and extract the value of ΔH_R, we performed titrations with 5 μL aliquots (which is the smallest volume that yields heat measurements with good accuracy). The high accuracy is reflected by the close to perfect reproducibility of the measured heat (Figure 3a), of all the injections (apart from the first injection which is ignored for the reasons explained

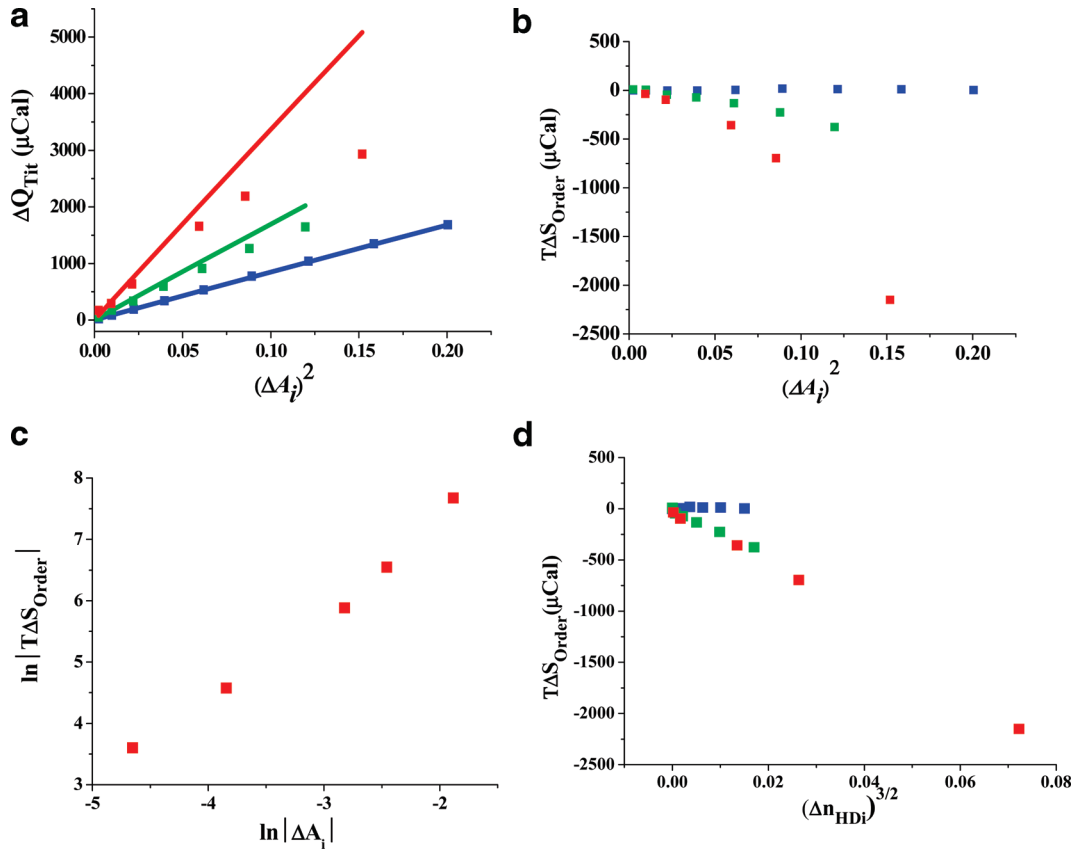

Figure 4. Experimental assessments of the entropic effects. (a) Measured total heat of titration ΔQ_{Tit} as a function of $(\Delta A_i)^2$ for dilution titrations in the stirring mode. The blue, green, and red squares correspond to titrations with 5, 10, and 20 μL volume aliquots, respectively. The blue, green and red solid lines are the corresponding computed values of ΔQ_{Reac}. (b) Corresponding values of $T\Delta S_{Order}$ that represent the deviations between the measured heat ΔQ_{Tit} and the computed values of ΔQ_{Reac}. (c) $\ln|T\Delta S_{Order}|$ as a function of $\ln|\Delta A_i|$, for 20 μL volume injected aliquots. (d) $T\Delta S_{Order}$ as a function of $(\Delta n_{HD,i})^{1.5}$ for all injected volumes.

in the Materials and Methods) and even for the titrations with very small mole fraction A.

As shown in Figure 3b, we found excellent agreement between the measured total heat ΔQ_{Tit} (integrated over each injection profile) as a function of $(\Delta A_i)^2$ and the calculated functional dependence ΔQ_{Reac} (using eq 11). Computation of the value of the enthalpy of reaction ΔH_R, from the experimental measurements (using eq 11), yielded 15.8 ± 0.3, 15.8 ± 0.3, 15.8 ± 0.3, and 15.7 ± 0.3 cal/mol for injections 2, 3, 4, and 5, respectively. Note that for each ith injection we averaged over 8 titrations with different mole fraction H_2O-D_2O solutions. These results are in a very good agreement with the earlier data[28] (ΔH_R = 15.5 cal/mol) obtained by using heat flux calorimetry.

The results shown in Figure 3a,b are for dilution titrations in the nonstirring mode. In Figure 3c we show that the same results are obtained when the titrations are performed using the stirring mode. In addition, we also performed the same set of experiments for concentration titrations, while using the stirring mode, and obtained the same results. These findings verify the theoretically computed functional dependence ΔQ_{Reac} on the mole fraction A.

In the Appendix, we further show that ΔQ_{Reac} mainly depends on the difference $\Delta A_i = |A_{i-1} - A_{Inj}|$ irrespective of the specific values of A_{i-1} and A_{Inj} (as long as A_{Inj} is smaller than 0.8). In other words, we can use H_2O-D_2O solutions for the titrations, instead of using H_2O as was done above and will obtain approximately the same results, provided the D/H ratios of the titrated and titrating solutions correspond to the same ΔA_i.

Experimental Assessments of the Entropic Effects. Once the functional dependence of the heat production ΔQ_{Reac} is confirmed, we can proceed to assess the entropy contributions ΔS_{Order} by titrations with lager volume aliquots. Along the explanations presented in the Introduction, deviations of the measured total heat of the titration ΔQ_{Tit}, from the computed values of ΔQ_{Reac} correspond to the entropy contributions resulting from deviations from ideal mixing. In simple words, at a certain temperature T

$$T\Delta S_{Order} \equiv \Delta Q_{Tit} - \Delta Q_{Reac} \qquad (13)$$

In Figure 4a we show the measured heat values of ΔQ_{Tit} as a function of $(\Delta A_i)^2$ for three dilution titrations with volumes, 5, 10, and 20 μL, while using the stirring mode. In Figure 4b we show the corresponding values of $T\Delta S_{Order}$ computed from the measurements according to eq 13.

Closer inspection (Figure 4c,d) of the measured entropy contribution $T\Delta S_{Order}$, revealed that it approximately scales as $(\Delta n_{HD,i})^{1.5}$ (and approximately as $(\Delta A_i)^3$). For a given value of the mole fraction change ΔA_i, $T\Delta S_{Order}$ scales approximately as the square of the injected volume ($T\Delta S_{Order} \sim V_{Inj}^2$). These observations of strong nonlinear dependence on the molar fraction and the volume support the idea that ΔS_{Order} might be the outcome of entropic effects that are associated with changes in the arrangements of the hydrogen bonds (see the Conclusions).

Comparison between Different Measurement Modes. In Figure 3c we showed that the same values of ΔQ_{Tit} (and hence

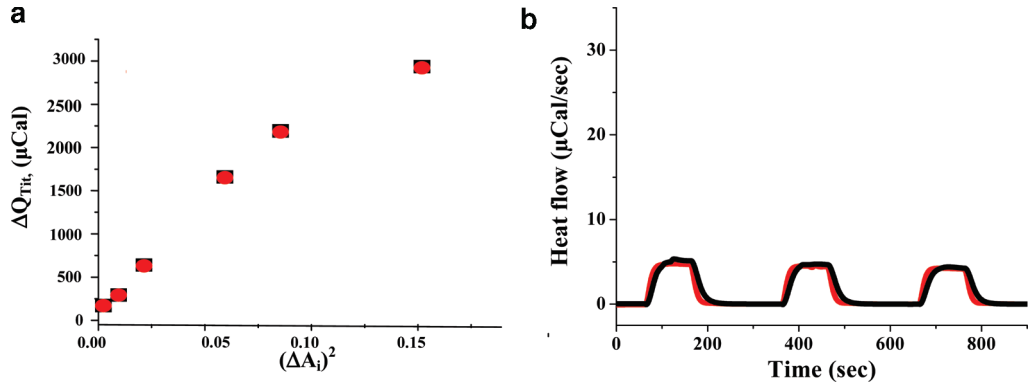

Figure 5. Comparison of the entropy deviations between different measurement modes. (a) Comparison between released heat for the nonstirring mode (red) and the stirring mode (black) for 10 μL dilution titrations. (b) Comparison of the heat flow during dilution titrations (red) and concentration titrations (black) for 50 μL titrations while using the stirring mode and for $|\Delta A_j| = 0.05$. We note that the shape of the measured heat flow might indicate heat saturation. However, the magnitudes of the measured heats are lower than the saturation level, as can be inferred from Figure 6b (much higher values of heat are measured). We also note that for this low value of 0.05 mol fraction difference between the injected and titrated solutions, the results (ΔQ_{Tit} per titration of approximately 500 μcal) are very close to the computed value of limit of ΔQ_{Reac} for ideal mixing.

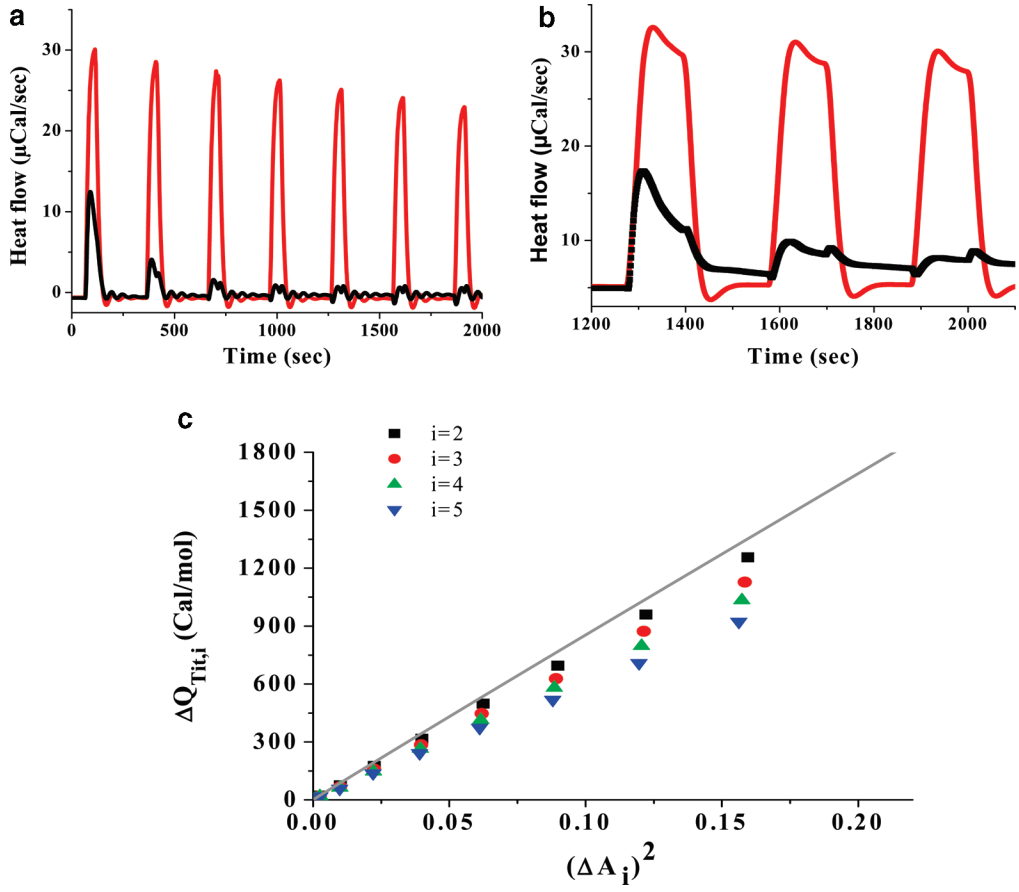

Figure 6. Heat flow during concentration titrations while using the nonstirring mode. (a) Comparison between the heat flow during concentration titrations while using the stirring mode (red) and the nonstirring mode (black) for $\Delta A_i = 0.2$ and 25 μL volume titration injections. (b) Comparison between the heat flow during concentration titrations (black) and dilution titrations (red) while using the nonstirring mode for $\Delta A_i = 0.2$ and 50 μL volume titration injections. (c) Measured heat $\Delta Q_{Tit,i}$ of injections 2, 3, 4, and 5 for different values of $(\Delta A_i)^2$, regarding concentration titrations. The solid black line is the corresponding calculated $\Delta Q_{Reac,i}$.

of ΔQ_{Reac}) are obtained while using the stirring and nonstirring mode in the case of low volume dilution titrations. In Figure 5a we show that similar deviations between ΔQ_{Tit} and ΔQ_{Reac} (and hence of $T\Delta S_{Order}$) are obtained while using the stirring and nonstirring mode in the case of dilution titrations. In addition, we also performed the same set of experiments for concentration titrations, while using the stirring mode, and obtained the same results as for the dilution titrations. In Figure 5b we show a comparison between the heat flows for the two types of titrations when high volume aliquots (50 μL) were used.

Experimental Assessments of the Reaction Kinetics of Concentration Titrations. In the case of concentration titrations, the nonstirring mode yields very different results from those obtained while using the stirring mode, as illustrated in Figure 6a. In Figure 6b we illustrate the difference between concentration titrations and dilution titrations when the non-

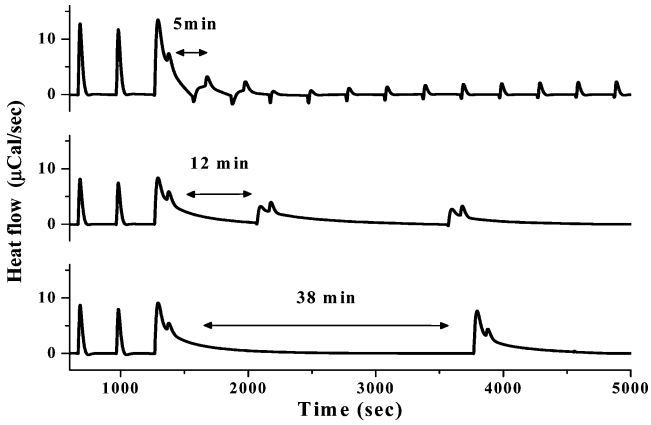

Figure 7. Estimation of the reaction kinetic times for concentration titrations. The experiment shows injections of a 20% D_2O-H_2O solution into H_2O. The first four 5 μL injections with 5 min delay time (between injections) are performed to check reproducibility (in the figures, we show the heat exchange profile of the last two of these 4 injections). Then 50 μL volume titration injections are performed (third and the following injections in the figures) with delay times between these injections of 5 min (top), 12 min (middle), and 38 min (bottom).

stirring mode is used. These results exemplify a significant reduction in the measured total heat ΔQ_{Tit} between successive volume concentration titrations while using the nonstirring mode. In Figure 6c we present quantified measures of the reductions in ΔQ_{Tit} for titrations with 5 μL volume injections. We note that even for such low volume titrations, the reduction in ΔQ_{Tit} is quite significant.

As mentioned earlier, in the case of concentration titrations, the reaction has to propagate throughout the apparatus cell whose volume is approximately 1.4 mL. Hence, the observed reduction in $\Delta Q_{\mathrm{Tit},i}$ between successive titrations might be indicative of long time reaction kinetic. To verify if this is the case and to estimate the characteristic times, we performed the ITC measurements for a range of delay times between the successive injections, as shown in Figure 7. We then define the characteristic time to be the minimum delay time between successive injections above which the heat exchange profile retains the same shape and magnitude as for the preceding injection. For the concentration titrations of 50 μL injection volume, shown in Figure 7, we estimated the kinetic time to be about 40 min.

We also performed similar experiments for dilution titrations and found, for large volume titrations (50 μL), that the kinetic times are of the order of 5 min. While these relaxation times are also quite long, the relaxation times for the concentration titrations are almost an order of magnitude longer (38 min).

The fact that the long kinetic times are observed for the nonstirring modes and are not observed for the stirring mode (which is the commonly used mode as it accelerates mixing) hints that they might be associated both with diffusion of the deuterium isotopes and with rearrangements of hydrogen bonds consequent to changes in the D/H ratios.

Conclusions

We presented accurate ITC measurements of the enthalpy of titration of D_2O-H_2O solutions with different D/H ratios for dilution and concentration titrations. The measurements were compared with theoretical calculations of the heat production ΔQ_{Reac} for 5 μL volume titrations. We found excellent agreement between the calculated and measured functional dependence of ΔQ_{Reac} and ΔQ_{Tit} on the D/H ratios of the solutions. Computation of the value of the enthalpy of reaction ΔH_{R}, from the experimental measurements, yielded a value of 15.8 ± 0.3 cal/mol for 1 mol of HDO formation. This result is in very good agreement with previous estimate of 15.5 cal/mol which was obtained using flow calorimetry.[28]

Next, we used larger volume titrations to asses the entropy contribution $T\Delta S_{\mathrm{Order}}$ (that is equal to the measured titration heat ΔQ_{Tit} minus the calculated one ΔQ_{Reac}). Since $\Delta S_{\mathrm{Order}}$ is a measure of deviations of entropy changes from the entropy change for ideal mixing, it is a measure of the changes in the bulk entropy of the H_2O-D_2O solution consequent to the titration induced changes in the D/H ratios. As such, $\Delta S_{\mathrm{Order}}$ provides an assessment of entropic effects associated with hydrogen bond rearrangements due to the changes in the D/H ratios. As noted earlier, this idea is further supported by our findings that $\Delta S_{\mathrm{Order}}$ approximately scales as $(\Delta n_{\mathrm{HD},i})^{1.5}$. Such nonlinear dependence of the bulk entropy on the mole fraction difference might be indicative that the network of hydrogen bonds has a fractal organization.

The measurements revealed significant negative (exothermic) values of $T\Delta S_{\mathrm{Order}}$. Such exothermic deviations from ideal mixing are indicative of excess entropy production during the titration. Several putative mechanisms can lead to such excess entropy increase. Recently there has been much focus on high density water (HDW) vs low density water (LDW) that correspond to the two possible orientations of two water molecules according to the hydrogen bonds[2,37,38] and are assumed not to be distributed uniformly. Thus, they can generate long-range correlations or ordering in the water (lower bulk entropy). In the presence of the three components, H_2O, D_2O, and DHO, there are additional possible orientations: 10 orientations for H_2O-H_2O, D_2O-H_2O, D_2O-D_2O, H_2O-HDO, and D_2O-HDO and 3 orientations for HDO$-$HDO. The formation of additional possible orientations should reduce the long-range ordering and hence be associated with higher bulk entropy. Therefore, one might expect an increase in entropy with an increase in the D/H ratio in the case of concentration titrations. Another putative source of entropy increase might be connected with ortho and para water that were suggested not to be distributed uniformly but to form clusters[11–13] and hence induce long-range ordering in the water (lower bulk entropy). Adding deuterium should destroy the long-range ordering associated with ortho and para water and thus result in excess entropy increase. We note that the two effects can act together, although so far the effect of ortho and para water on the HDW and LDW has not been studied.

The observed long kinetic times are consistent with the aforementioned picture for the following reasons: Water molecules are connected by a network of hydrogen bonds. This network is very dynamic and the hydrogen bonds continuously rearrange.[39,40] When there is no mechanical mixing (we performed the kinetic experiment using the nonstirring mode), the propagation (diffusion or hopping) of the deuterium is likely to be the main mechanism by which D_2O and H_2O molecules mix. This is in accordance with other findings that showed D_2O molecules hold together as clusters and do not mix readily with H_2O molecules.[41]

To estimate the hopping rate of the deuterium, we note that the hopping distance is about 2−3 Å (a typical distance between hydrogen atoms) and the hopping time is about 10 ps (the lifetime of the hydrogen bond). Since the size of the sample cell is about 1 cm, we find that the propagation time is of the

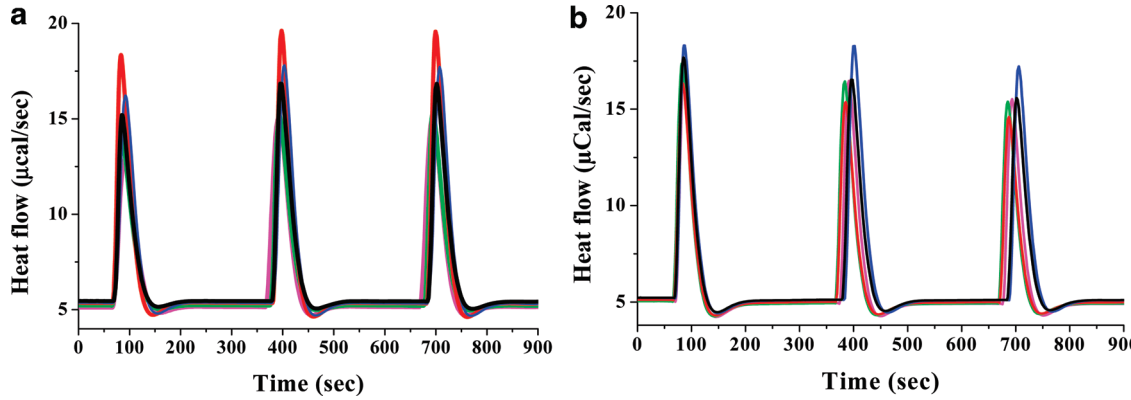

Figure A1. Heat flows for the dilution and concentration titrations, when $\Delta A_i = |A_{i-1} - A_{\mathrm{Inj}}| = 0.2$; $V_{\mathrm{Inj}} = 5\ \mu$L, 303 K, nonstirring, high feedback. (a) Dilution titrations for $A_{i-1} = 0.2$ (black), 0.4 (blue), 0.6 (red), 0.8 (green), and 1.0 (pink) and $A_{\mathrm{Inj}} = 0.0$, 0.2, 0.4, 0.6, and 0.8 respectively. (b) Concentration titrations for $A_{\mathrm{Inj}} = 0.2$ (black), 0.4 (blue), 0.6 (red), 0.8 (green), and 1.0 (pink) and $A_{i-1} = 0.0$, 0.2, 0.4, 0.6, and 0.8, respectively.

order of 1000−2000 s, which is consistent with the experimentally estimated measured 40 min kinetic time.

To conclude, we observed significant entropy contributions that might be associated with nontrivial entropic effects that are related to the D/H ratios of the D_2O-H_2O solutions. Since the entropic effects are likely to be associated with the D/H dependence of the hydrogen bond rearrangements, and since we observed long reaction propagation times, our experimental findings might be associated with the existence of long-range water ordering. We emphasize that the results presented here are consistent with this intriguing putative explanation. However, additional complementary experiments, such as near-infrared spectroscopy[42] and electrophoretic mobility (ζ-potential) of D_2O-H_2O solutions with different D/H ratios, are required for sound validation of this notion.[43,44]

Acknowledgment. The research presented here has been supported in part by the Maguy-Glass Chair in Physics of Complex Systems at Tel Aviv University, the Tauber Family Foundation, and a grant from the Fetzer Institute.

Appendix: Analytical Approximation of Equation 4

Taylor expansion of eq 4 yields

$$X_{\mathrm{HD}} = 2A(1-A) - 2\left(\frac{4}{K} - 1\right)A^2(1-A)^2 + 4\left(\frac{4}{K} - 1\right)^2 A^3(1-A)^3 + \ldots \quad \text{(Ai)}$$

By neglecting the second and third terms, whose magnitude is less than 1% of the first term, and using the definition of $\Delta n_{\mathrm{HD},i}$ (eq 9), we obtained

$$\Delta n_{\mathrm{HD},i} = \frac{2n_{i-1}n_{\mathrm{Inj}}(A_{i-1} - A_{\mathrm{Inj}})^2}{n_{i-1} + n_{\mathrm{Inj}}} \quad \text{(Aii)}$$

This result indicates that ΔQ_{Reac} (and also the titration heat ΔQ_{Tit}) mainly depends on the difference $|A_{i-1} - A_{\mathrm{Inj}}|$ irrespective of the specific values of A_{i-1} and A_{Inj} as long as A_{Inj} is not too large. In Figure A1 we show comparison between the heat flows of different values of A_{i-1} and A_{Inj}, while keeping the same value of $|A_{i-1} - A_{\mathrm{Inj}}| = 0.2$. The results reveal that indeed for A_{Inj} smaller than 0.8, the measured heats ΔQ_{Tit} are similar irrespective of the specific values of A_{i-1} and A_{Inj}.

References and Notes

(1) Ball, P. Water: Water - an enduring mystery. *Nature* **2008**, *452*, 291–292.
(2) Debenedetti, P. G.; Stanley, H. E. Supercooled and Glassy Water. *Phys. Today* **2003**, *56* (6), 40–46.
(3) Franks, F. *Water A Comprehensive Treatise(1−6)*; Plenum Press: New York, 1972−1979.
(4) Stillinger, F. H. Water Revisited. *Science* **1980**, *209*, 451–7.
(5) Gordon, T. H.; Hura, G. Water Structure from scattering experiments and simulation. *Chem. Rev* **2002**, *102*, 2651–2670.
(6) Ball, P. *Life's matrix: a biography of water*, 1st ed.; Farrar Straus and Giroux: New York, 2000.
(7) Pershin, S. M. Two-liquid water. *Phys. Wave Phenom.* **2005**, *13*, 192–208.
(8) Pershin, S. M. Harmonic Oscillations of the Concentration of H-bonds in Liquid Water. *Laser Phys.* **2006**, *16*, 1184–1190.
(9) Soper, A. K.; Ricci, M. A. Structures of High-Density and Low-Density Water. *Phys. Rev. Lett.* **2000**, *84* (13), 2881–2884.
(10) Chae, U. K.; Barstowb, B.; Tatec, M. W.; Gruner, S. M. Evidence for liquid water during the high-density to low-density amorphous ice transition. *Proc. Natl. Acad. Sci. U.S.A.* **2009**, *106*, 4596–4600.
(11) Potekhin, S. A.; Khusainova, R. S. Spin-dependent absorption of water molecules. *Biophys. Chem.* **2005**, *118*, 84–87.
(12) Pershin, S. M. Coincidence of rotational energy of H_2O ortho-para molecules and translation energy near specific temperatures in water and ice. *Phys. Wave Phenom.* **2008**, *16*, 15–25.
(13) Andreev, S. N.; Makarov, V. P.; Tikhonov, V. I.; Volkov, A. A. Ortho and Para Molecules of Water in Electric Field. arXiv:physics/0703038v12007.
(14) Chaplin, M. F. Opinion: Do we underestimate the importance of water in cell biology. *Nat. Rev. Mol. Cell Biol.* **2006**, *7* (11), 861–866.
(15) Pollack, G. H. *Cells, Gels and the Engines of Life: A New, Unifying Approach to Cell Function*: Ebner & Sons: Seattle, WA, 2001.
(16) Harris, K. R. Isotope effects and the thermal offset effect for diffusion and viscosity coefficients of liquid water. *Phys. Chem. Chem. Phys.* **2002**, *4*, 5841–5845.
(17) Lopez, M. M.; Makhatadze, G. I. Solvent isotope effect on thermodynamics of hydration. *Biophys. Chem.* **1998**, *74* (2), 117–125.
(18) Graziano, G. On the solvent isotope effect in hydrophobic hydration. *J. Phys. Chem. B* **2000**, *104*, 9249–9254.
(19) Marcus, Y.; Ben-Naim, A. A study of the structure of water and its dependence on solutes, based on the isotope effects on solvation thermodynamics in water. *J. Chem. Phys.* **1985**, *83*, 4744–4759.
(20) Jelinska-Kazimierczuk, M.; Szydlowski, J. Physicochemical Properties of Solutions of Amides in H_2O and in D_2O. *J. Solution Chem.* **2001**, *30*, 623–640.
(21) Wolf, D.; Kudish, A. I. Effect of isotope substitution on the viscosity of water-methanol mixtures at 25 °C. *J. Phys. Chem.* **1980**, *84*, 921–925.
(22) Chumaevskii, N. A.; Rodnikova, M. N.; Sirotkin, D. A. Raman spectra of light and heavy water in the O-H and O-D stretching vibrations region. *J. Mol. Liq.* **1999**, *82*, 39–46.

(23) Avila, G.; Tejeda, G.; Fernandez, J. M.; Montero, S. The Raman spectra and cross-sections of the band of HO, DO, and HDO. *J. Mol. Spectrosc.* **2004**, *223*, 166–180.

(24) Hiroko, M.; Satoshi, H.; Hiroshiga, K.; Hiro-o, H. Raman spectra indicative of unusual water structure in crystals formed from a room-temperature ionic liquid. *J. Raman Spectrosc.* **2006**, *37*, 1242–1243.

(25) Weingartner, H.; Chatzidimttriou-Dreismann, C. A. Anomalous H^+ and D^+ conductance in H_2O-D_2O mixtures. *Nature* **1990**, *346*, 548–550.

(26) Biondi, C.; Bellugi, L. Diffusion of some species of different charge and mass in light and heavy water. *Chem. Phys.* **1981**, *62*, 145–152.

(27) Milhaud, J.; Hantz, E.; Liquier, J. Different Properties of H_2O and D_2O-Containing Phospholipid-Based Reverse Micelles near a Critical Temperature. *Langmuir* **2006**, *22*, 6068–6077.

(28) Simonson, J. M. The enthalpy of the isotope-exchange reaction: $H_2O + D_2O = 2HDO$ at temperatures to 673K and at pressures to 40 MPa. *J. Chem. Thermodyn.* **1990**, *22*, 739–749.

(29) Matulis, D.; Bloomfield, V. A. Thermodynamics of the Hydrophobic Effect. II. Calorimetric Measurement of Enthalpy, Entropy, and Heat Capacity of Aggregation of Alkylamines and Long Aliphatic Chains. *Biophys. Chem.* **2001**, *93*, 53–65.

(30) Valezquez-Campoy, A.; Leavitt, S. A.; Feire, E. Characterizition of protein-protein interactions by isothermal titration Calorimetry. *Methods Mol. Biol.* **2004**, *261*, 35–54.

(31) Wiseman, T. S.; Brandts Williston, J. F.; Lin, L. N. Rapid measurement of binding constants and heats of binding using a new titration calorimeter. *Anal. Biochem.* **1989**, *179*, 131.

(32) Traut, T. W. Dissociation of enzyme oligomers: a mechanism for allosteric regulation. *Crit. Rev. Biochem. Mol. Biol.* **1994**, *29*, 125–163.

(33) Burrows, S. D.; Doyle, M. L.; Murphy, K. P.; Franklin, S. G.; White, J. R.; Brooks, I.; McNulty, D. E.; Scott, M. O.; Knutson, J. R.; Porter, D.; Young, P. R.; Hensley, P. Determination of the monomer-dimer equilibrium of interleukin-8 revelas it is a monomer at physiological concentrations. *Biochemistry* **1994**, *33*, 12741–12745.

(34) Lovatt, M.; Cooper, A.; Camilleri, P. Energetics of cyclodextrin-induced dissociation of insulin. *J. Eur. Biophys* **1996**, *24*, 354–357.

(35) Shinitzky, M.; Shvalb, A.; Elitzur, A. C.; Mastai, Y. Entrapped energy in chiral solutions: Quantification and information capacity. *J. Phys. Chem. B* **2007**, *111*, 11004–11008.

(36) Dimova, R.; Lipowsky, R.; Mastai, Y.; Antonietti, M. Binding of polymers to calcite crystals in water: Characterization by isothermal titration calorimetry. *Langmuir* **2003**, *19*, 6097–6103.

(37) Stanley, H. E.; Kumar, P.; Franzese, G.; Xu, L.; Yan, Z.; Mazza, M. G.; Buldyrev, S. V.; Chen, S. H.; Mallamace, F. Liquid Polyamorphism: Possible Relation to the Anomalous Behavior of Water. *Eur. Phys. J.: Special Topics* **2008**, *161*, 1–17.

(38) Yan, Z.; Buldyrev, S. V.; Kumar, P.; Giovambattista, N.; Debenedetti, P. G.; Stanley, H. E. Structure of the First- and Second-Neighbor Shells of Simulated Water: Quantitative Relation to Translational and Orientational Order. *Phys. Rev. E* **2007**, *76*, 051201(1)–051201(5).

(39) Keutsch, N. F.; Saykally, R. J. Water clusters: Untangling the mysteries of the liquid, one molecule at a time. *Proc. Natl. Acad. Sci. U.S.A.* **2001**, *98*, 10533–10540.

(40) Fellers, R. S.; Leforestier, C.; Braly, L. B.; Brown, M. G.; Saykally, R. J. Spectroscopic determination of the water pair potential. *Science* **1999**, *284*, 945–948.

(41) Gorman, W. R.; Brownridge, J. D. Reduced heat flow in light water (H_2O) due to heavy water (D_2O). *Appl. Phys. Lett.* **2008**, *93*, 034101(1)–034101(3).

(42) Tsenkova, R. AquaPhotomics: water absorbance pattern as a biological marker for disease diagnosis and disease understanding. *J. Near Infrared Spectrosc.* **2008**, *18*, 14–16.

(43) Seebergh, J. E.; Berg, J. C. The Effect of Organic Cosolvent on the Aggregation Stability of an Aqueous Polystyrene Latex Dispersion. *Colloids Surf. A* **1997**, *121*, 89–98.

(44) El-Gholabzouri, O.; Cabrerizo, M. A.; Hidalgo-Álvarez, R. Streaming Current of Polystyrene Porous Plugs: Solvent Composition Effect. *J. Colloid Interface Sci.* **1998**, *199*, 38–43.

JP909657M